PELI2 regulates early B-cell progenitor differentiation and related leukemia via the IL-7R expression

Yan Xu,[1,2,3] Qian Zhou,[1,2,3] Xiaoming Wang,[4] Aijun Zhang,[4] Wentao Qi,[1,2,3] Yuan Li,[1,2,3] Chengzu Zheng,[1,2,3] Jianmin Guan,[5] Tao Sun,[6] Jingxin Li,[7] Chunhua Lu,[1,2] Yuemao Shen[1,2] and Baobing Zhao[1,2,3]

[1]Key Lab of Chemical Biology (MOE), School of Pharmaceutical Sciences, Cheeloo College of Medicine, Shandong University, Jinan; [2]NMPA Key Laboratory for Technology Research and Evaluation of Drug Products, School of Pharmaceutical Sciences, Cheeloo College of Medicine, Shandong University, Jinan; [3]Department of Pharmacology, School of Pharmaceutical Sciences, Cheeloo College of Medicine, Shandong University, Jinan; [4]Department of Pediatrics, Qilu Hospital of Shandong University, Jinan; [5]Department of Hematology, Heze Municipal Hospital, Heze; [6]Department of Hematology, Qilu Hospital of Shandong University, Jinan and [7]Department of Physiology, School of Basic Medical Sciences, Cheeloo College of Medicine, Shandong University, Jinan, Shandong, China

Correspondence: B. Zhao
baobingzh@sdu.edu.cn

Received: August 6, 2023.
Accepted: November 24, 2023.
Early view: December 7, 2023.

https://doi.org/10.3324/haematol.2023.284041

Abstract

Little is known about the transition mechanisms that govern early lymphoid lineage progenitors from common lymphoid progenitors (CLP). Pellino2 (*PELI2*) is a newly discovered E3 ubiquitin ligase, which plays important roles in inflammation and the immune system. However, the physiological and molecular roles of *PELI2* in the differentiation of immune cells are largely unknown. Here, by using a conditional knockout mouse model, we demonstrated that *PELI2* is required for early B-cell development and stressed hematopoiesis. *PELI2* interacted with and stabilized PU.1 via K63-polyubiquitination to regulate IL-7R expression. The defects of B-cell development induced by *PELI2* deletion were restored by overexpression of PU.1. Similarly, *PELI2* promoted TCF3 protein stability via K63-polyubiquitination to regulate IL-7R expression, which is required for the proliferation of B-cell precursor acute lymphoblastic leukemia (BCP-ALL) cells. These results underscore the significance of *PELI2* in both normal B lymphopoiesis and malignant B-cell acute lymphoblastic leukemia via the regulation of IL-7R expression, providing a potential therapeutic approach for BCP-ALL.

Introduction

B-cell development arises from the commitment of hematopoietic stem cells (HSC) into common lymphoid progenitors (CLP) and subsequent B-cell lineage specification in the bone marrow (BM).[1] CLP include two distinct populations: an all-lymphoid progenitor (ALP) subset that retains full lymphoid potential and early thymic seeding activity, and a B-cell-biased lymphoid progenitor (BLP) population that primarily acts as an early B-cell progenitor pool.[2] Early B-cell progenitors progressively differentiate through well-defined intermediates before they migrate to peripheral lymphoid tissues for the functional activation in response to antigen exposure, including pre-pro-B cells, pro-B cells, pre-B cells, immature B cells, and mature B cells stages.[1,3] This process is characterized by the sequential expression of B-cell gene program and V(D)J recombination events, and is controlled by a network of transcription factors including PU.1, Ikaros, E2A, Ebf1, and Pax5.[3,4] Mutations or alterations of these transcription factors represent an underlying cause of phenotypic features such as the developmental arrest observed in B-cell precursor acute lymphoblastic leukemia (BCP-ALL).[5]

Several signaling events via transmembrane receptors are critical for B-cell lineage development.[6-9] Among them, IL-7R signaling not only plays essential roles in B-cell lineage specification from CLP, but is also required for the survival and proliferation of early B-cell progenitors.[10,11] IL-7R is a heterodimer formed by the IL-7Rα-chain (IL-7Rα) and a common γ chain (γc).[8] Binding of IL-7 to IL-7R initiates phosphorylation of JAK1 and JAK3, which recruits and activates downstream signal transducer and activator of transcription (STAT) as well as PI3K/Akt/mTOR and MEK-ERK pathways. These signalings co-operatively activate a B-cell lineage gene expression program including Pax5, Ebf1, and BCL-2 family proteins.[7] Deficiencies in the IL-7R signaling in mice or humans result in severe lymphopenia.[12-15] The importance of keeping *IL*-7R-mediated signaling

under control is also illustrated by studies showing that IL-7 transgenic mice develop B-cell lymphomas, and that IL-7 induces proliferation of BCP-ALL cells.[16] Furthermore, most recent studies have demonstrated that IL-7R mutational activation is sufficient to trigger BCP-ALL.[17,18]

Pellino2 (*PELI2*) is a newly discovered E3 ubiquitin ligase, which regulates the protein degradation, protein-protein interaction, protein translocation and signaling transduction via the ubiquitination of target proteins.[19] *PELI2* possesses a C-terminal RING-like domain and a phospho-threonine-binding forkhead-associated (FHA) domain that are responsible for ubiquitin ligase activity and substrate binding, respectively.[20] There is growing evidence that *PELI2* acts as a critical mediator for innate immunity via multiple signalings through IL-1 receptors, Toll-like receptors, and NOD-like receptors.[21,22] However, the physiological and molecular roles of *PELI2* in the development of immune cells are largely unknown. Here, we generated and characterized a conditional knockout mouse model in which *PELI2* was specifically depleted in hematopoietic cells. We found that *PELI2* was required for early B-cell development, the deficiency of which resulted in a defect of the B-cell progenitors committed from CLP. Furthermore, *PELI2* promoted the proliferation of BCP-ALL cells via the expression of IL-7R.

Methods

Mice

PELI2 floxed mice (*PELI2*$^{fl/fl}$) were generated by inserting loxp sites flanking exon 2, which when deleted results in a frame-shift and form a premature stop codon in the reading frame. All animal studies were approved by the Institutional Animal Care and Use Committees at Shandong University.

Human BCP-ALL xenograft

Nalm-6 cells xenografts were carried out as previously described.[23] The 6-week-old male NSG mice (Charles River Laboratories, Beijing, China) were irradiated at 1 Gy before tail vein injection of 5x10^6 Nalm-6 cells infected with object virus.

Chromatin immunoprecipitation

Chromatin immunoprecipitation (ChIP) assays were performed as previously described.[24] Cells were fixed and lysed using a SimpleChIP Enzymatic Chromatin IP Kit (Cell Signaling Technology) according to the manufacturer's protocol.

Statistical analysis

Statistical analyses were performed with unpaired two-tailed Student *t* test except where indicated otherwise using Prism (GraphPad). $P<0.05$ was considered statistically significant.

Additional methods and detailed information are provided in the *Online Supplementary Appendix*.

Results

PELI2 was required for early B-cell development

To explore the physiological roles of *PELI2* in hematopoiesis, we generated a conditional *PELI2* knockout model. Mice bearing *PELI2* allele with loxP-flanked exon 2 (*PELI2*$^{fl/fl}$) were crossed with Vav-Cre transgenic mice, to generate hematopoietic-specific *PELI2* knockout mice (*PELI2*$^{fl/fl}$; Vav-cre, CKO) with a deletion of the exon 2 (*Online Supplementary Figure S1A*). The deletion of *PELI2* expression was confirmed by qPCR assays in the mononuclear cells from BM (*Online Supplementary Figure S1B*). The mice with *PELI2* deficiency did not differ in morphology, growth, or viability from their wild-type (WT) littermates (*data not shown*). However, CKO mice clearly exhibited leukopenia, as demonstrated by the reduced white blood cells but unaffected red blood cells and platelets in the peripheral blood (PB) (Figure 1A, *Online Supplementary Figure S1C*). In addition, the reduced numbers of lymphocytes accounted for the leukopenia phenotype in the CKO mice, which was mainly caused by the reduction in B cells (B220$^+$) in the PB (Figure 1A, B, *Online Supplementary Figure S1D*).

We then examined the B-cell compartment in BM, the primary tissue in which early B-cell development occurs. The frequency and numbers of B cells (B220$^+$) in BM was significantly decreased in CKO mice compared to that in WT mice (Figure 1C, D, *Online Supplementary Figure S1E*), while other lineage cells including T cells appeared normal in CKO mice (*date not shown*). Similarly, CKO mice also showed reduced numbers of B cells in the spleen, as well as a mild decrease in spleen weight (*Online Supplementary Figure S1F, G*). Although T cells were also reduced in CKO mice spleen, the early T-cell development in thymus was for the most part normal in CKO mice (*Online Supplementary Figure S1H, I*).

To clarify the defect in B-cell development upon the *PELI2* deletion, we examined the subpopulations of B cells. The frequencies of pro-B cells and pre-B cells were slightly reduced in *PELI2*^{CKO} BM while mature B cells showed a slight increase, indicating that *PELI2* deficiency disrupted the sequential differentiation bias of B-cell progenitors (defined as B220$^+$IgM$^-$IgD$^-$) (*Online Supplementary Figure S1J*). Notably, all the subpopulations of B cells were reduced in *PELI2*^{CKO} BM compared to WT controls (*Online Supplementary Figure S1J*). Although HSC (Lin$^-$Sca1$^+$c-Kit$^+$) and HPC (Lin$^-$Sca1$^-$c-Kit$^+$) were not apparently compromised in CKO mice (*Online Supplementary Figure S1K*), CLP in CKO BM were significantly reduced compared to that of WT mice (Figure 1E, F). Using the surface marker Ly6D, we further divided CLP into ALP (Ly6D$^-$) and BLP (Ly6D$^+$) populations[2] (Figure 1E). Compared to the equal numbers of ALP cells, the absolute BLP cells that primarily act as

early B-cell progenitors were significantly reduced in CKO mice (Figure 1G). This was further confirmed by the colony-forming assays with CKO BM Lin$^-$ cells supplemented with IL-7, which showed that the colony number and size were significantly reduced from CKO BM cells (Figure 1H). These findings suggested that *PELI2* is required for the commitment and proliferation of B-biased lymphoid progenitor cells from CLP.

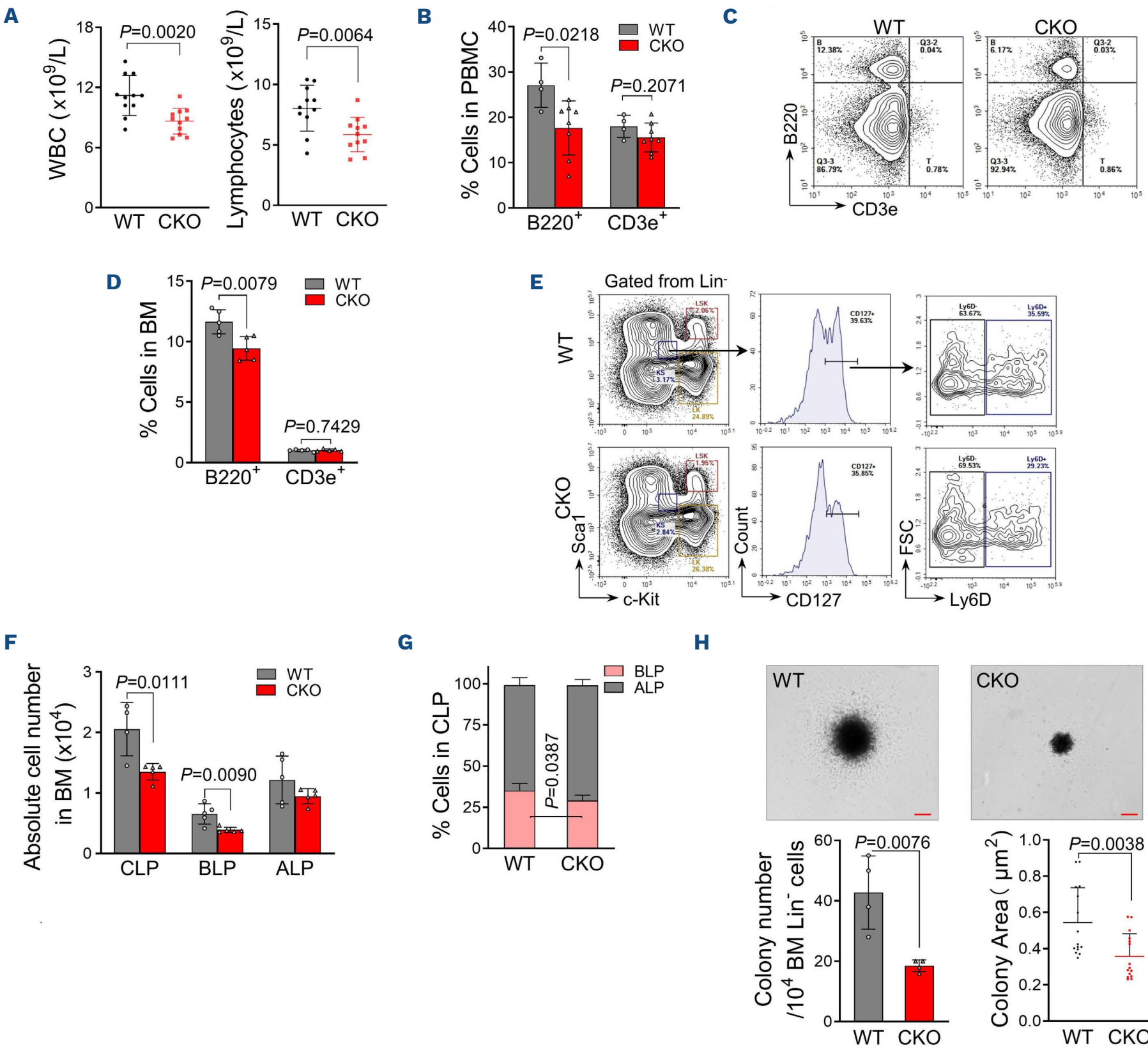

Figure 1. *PELI2* deficiency impairs early B-cell development. (A) Peripheral blood analysis of wild-type (WT) and 8-week old *PELI2*^{CKO} mice (CKO) (N=11). Data presented as mean±Standard Deviation (SD). (B) Quantification of B cells (B220$^+$) and T cells (CD3e$^+$) in the peripheral blood mononuclear cells (PBMC) from mice as in (A). Each dot represents one mouse. Data presented as mean±SD. (C) Representative flow cytometric analysis of B cells and T cells in the bone marrow (BM) of 8-week-old WT and *PELI2*^{CKO} mice. (D) Quantification of the percentage of B cells and T cells in (C). Each dot represents one mouse. Data presented as mean±SD. (E) Representative flow cytometric analysis of common lymphoid progenitor (CLP) cells, B-cell-biased lymphoid progenitor (BLP) cells, and all-lymphoid progenitor (ALP) cells in the BM of 8-week-old WT and *PELI2*^{CKO} mice. (F) Quantification of the numbers of CLP cells, BLP cells and ALP cells in (E). Each dot represents one mouse. Data presented as mean±SD. (G) Quantification of the percentage of BLP cells and ALP cells in the BM from indicated mice as in (E) (N=5). Data presented as mean±SD. (H) Pre-B-colony formation assays of BM lineage$^-$ cells from WT and *PELI2*^{CKO} mice (N=4). Data presented as mean±SD. (Top) Representative colony morphology on day 7. Scale bar: 50μm. (Bottom) Colony number and size was quantified. All *P* values were determined by unpaired two-tailed Student *t* test unless otherwise indicated. See also *Online Supplementary Figure S1* for supporting information. CKO: hematopoietic-specific *PELI2* knockout mice (*PELI2*$^{fl/fl}$; Vav-cre).

Loss of *PELI2* impaired the reconstitution capacity of hematopoietic stem cells

To test whether a B-cell defect is the cell-intrinsic effect of HSC, we performed BM transplantation assays in which WT or CKO BM cells were transplanted into the lethally irradiated mice (Figure 2A). CKO-BM reconstituted mice exhibited persistently low lymphocyte counts but other blood cell values were normal at four months post transplantation (Figure 2B, *Online Supplementary Figure S2A*). The frequency of B cells was also significantly reduced in PB, BM and spleen of CKO-BM reconstituted mice (Figure 2C). Furthermore, CKO-BM reconstituted mice showed reduced CLP compared to WT controls (Figure 2D).

Although the total LSK ($Lin^-Sca1^+c\text{-}Kit^+$) cells were comparable (*data not shown*), the numbers of SLAM-LSK ($CD150^+CD48^-LSK$) indicating the enriched HSC were significantly decreased in CKO-BMT mice (*Online Supplementary Figure S2B*). Correspondingly, *PELI2* deficiency led to the increased quiescence in SLAM-LSK (*Online Supplementary Figure S2C*). To examine the effect of *PELI2* deficiency on HSC functions, we challenged the CKO mice with 5-fluorouracil (5-FU) that induces the cell death of cycling HSPC to activate and mobilize HSC.[25] CKO mice exhibited a significant decrease in LSK expansion upon 5-FU administration (Figure 2E), and succumbed to BM failure significantly earlier than their WT littermates (Figure 2F). Moreover, we further assessed the absolute number of functional HSC with limiting-dilution assays and observed an approximately 2.5-fold reduction in HSC in CKO mice (Figure 2G). These findings suggest that *PELI2* is required for the self-renewal of HSC in stressed hematopoiesis.

To further confirm the functional roles of *PELI2* in HSC, we performed competitive BM transplantation assays (*Online Supplementary Figure S2F*). $PELI2^{CKO}$-derived cells showed a progressive decrease in PB in the primary transplant recipients, coinciding with a significantly impaired reconstitution in the BM (Figure 2H, I). However, $PELI2^{CKO}$ HSC were efficiently engrafted in the recipient BM as the WT controls indicated by homing assays (*Online Supplementary Figure S2D, E*). Notably, $PELI2^{CKO}$ HSC exhibited dramatically impaired proliferation but no relevant alteration in the lineage commitments in the recipient mice (Figure 2J, *Online Supplementary Figure S2G*). The competitive disadvantage of $PELI2^{CKO}$ HSC reconstitution was persistent in subsequent secondary recipients (*Online Supplementary Figure S2H, I*), indicating the defective self-renewal of HSC in $PELI2^{CKO}$ mice.

To rule out the possibility that the defect of $PELI2^{CKO}$ mice is due to a long-term accumulated consequence from the embryo stage, we also evaluated the role of *PELI2* in adult hematopoiesis, using chimeric mice transplanted with $PELI2^{fl/fl}$; Ubc-cre-ERT2 BM. Similar to $PELI2^{CKO}$ mice, *PELI2* deletion after injection of tamoxifen also impaired the reconstitution capacity of HSC and early B-cell development in adult mice (*Online Supplementary Figure S3*).

PELI2 regulated early B-cell development through IL-7R signaling pathway

The reduced pool of $B220^+$ cells and BLP in $PELI2^{CKO}$ mice prompted us to investigate the basis of impaired B-cell development. Loss of *PELI2* led to a slight increase in cell death in $B220^+$ BM cells, whereas $PELI2^{CKO}$ CLP showed comparable survival to WT (*Online Supplementary Figure S4A, B*). Importantly, B-cell proliferation *in vivo* was markedly restrained upon the *PELI2* deletion indicated by BrdU incorporation assays (Figure 3A). In line with this, the expression of *ccnd3*, a proliferation-related gene, was significantly reduced in $PELI2^{CKO}$ CLP and $B220^+$ BM cells (Figure 3B). These data indicated that the B-cell defect observed in $PELI2^{CKO}$ mice was mainly due to the inhibition of early B-cell progenitor cell proliferation.

To understand the molecular mechanism underlying the impaired B-cell development induced by *PELI2* deficiency, we performed bulk RNA sequencing of $B220^+$ BM cells from $PELI2^{CKO}$ mice and their WT controls. A total of 537 differentially expressed genes (DEG) were found (≥1.5-fold, $P<0.05$), including transcription factors related to early B-cell development such as EBF1, FOXO1, and PAX5 (Figure 3C). These genes were also confirmed to be markedly down-regulated in the CLP as well as $B220^+$ BM cells from $PELI2^{CKO}$ mice (Figure 3D, *Online Supplementary Figure S4C*). IL-7R, the key factor for early B-cell differentiation, was also down-regulated upon *PELI2* deletion, which was further confirmed by its notably reduced expression and surface protein level in the $PELI2^{CKO}$ CLP (Figure 3D, E). As expected, loss of *PELI2* led to the inhibition of IL-7R signaling, as indicated by the reduced phosphorylation of Stat5 and AKT (Figure 3F, G). Although signals from IL-7R were shared in B/T cell-biased lymphoid progenitors from CLP, *PELI2* deletion had no effect on the T-cell specific genes, including *E2AE47*, *HES1*, and *NOTCH1* (*Online Supplementary Figure S4D*).

To further confirm the critical role of IL-7R in the *PELI2* loss-of-function phenotype, we performed rescue experiments in which $PELI2^{CKO}$ $cKit^+$ BM cells transduced with lentivirus expressing IL-7R were transplanted into recipient mice. As we expected, IL-7R overexpression significantly reversed the defect of B-cell differentiation in $PELI2^{CKO}$ mice, indicated by the increased number of $B220^+$ cells and BLP in BM and spleen accompanied by the high levels of lymphocytes in PB (Figure 3H, I, *Online Supplementary Figure S4E, F*).

PELI2 regulated IL-7R expression via PU.1 ubiquitination in early B-cell development

Several transcription factors have been seen to control the expression of IL-7R, including PU.1, RUNX1, and GA-binding protein transcription factor.[26] Although the mRNA level of PU.1 was unaltered, its protein level was clearly reduced in *PELI2*-deficient $B220^+$ BM cells (Figure 4A, *Online Supplementary Figure S5A*). In line with this, PU.1 target gene

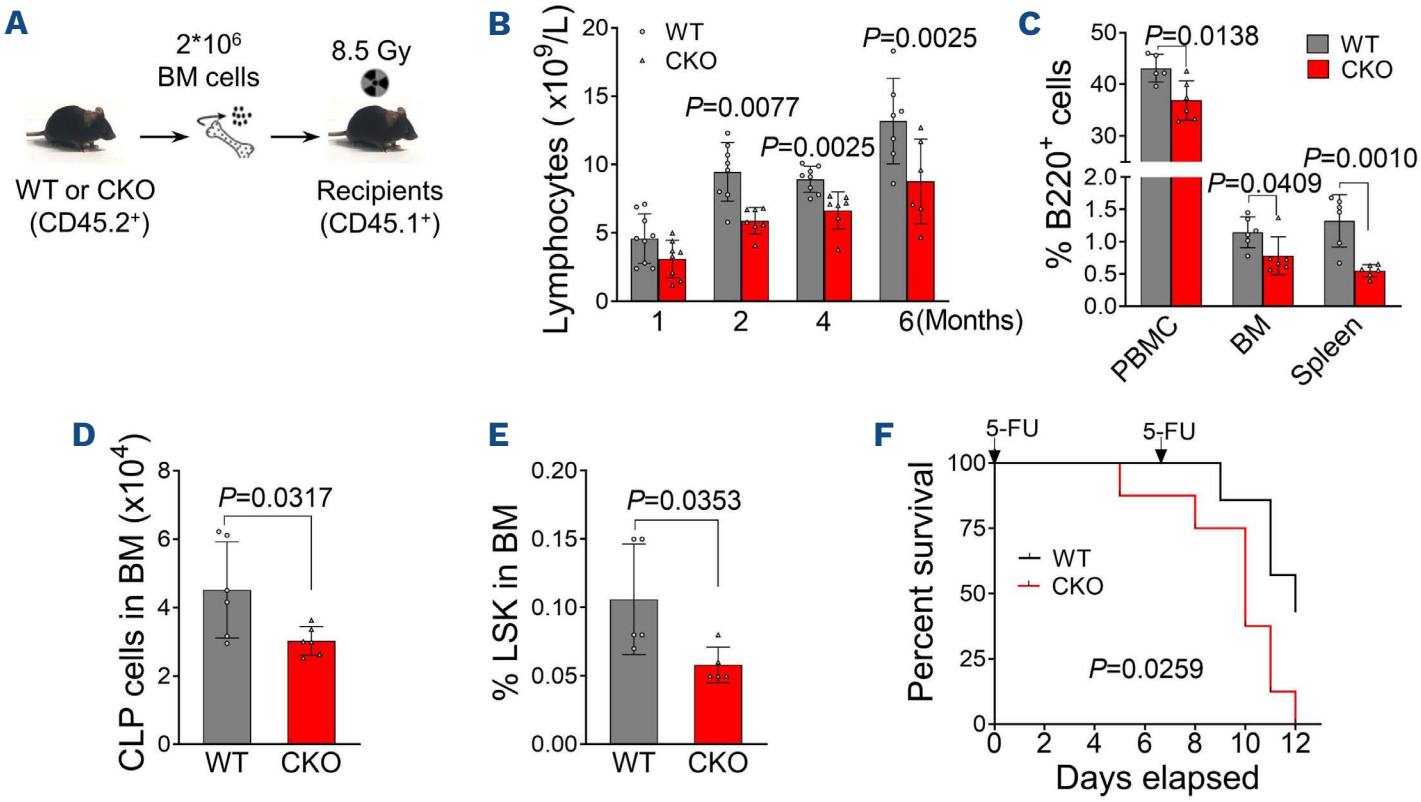

Figure 2. B lymphopenia in *PELI2*^{CKO} mice was cell autonomous. (A) Schematic illustration of serial bone marrow (BM) transplantation with wild-type (WT) and hematopoietic-specific *PELI2* knockout (*PELI2*^{CKO}) (CKO) mice BM cells. (B) Peripheral blood (PB) chimerism analyses at the indicated time points after 1st non-competitive BM transplantation. Each dot represents one mouse. Data presented as mean±Standard Deviation (SD). (C) Percentage of B cells in the peripheral blood mononuclear cells (PBMC), BM, and spleen of indicated mice 24 weeks after BM transplantation. Each dot represents one mouse. Data presented as mean±SD. (D) Numbers of common lymphoid progenitor (CLP) cells in the BM of indicated mice as in (C). Each dot represents one mouse. Data presented as mean±SD. (E) Quantification of LSK cells in the BM of WT and *PELI2*^{CKO} mice 8 days after 5-fluorouracil (5-FU, 150 mg/kg) treatment via single intraperitoneal injection. Each dot represents one mouse. Data presented as mean±SD. (F) Kaplan-Meier survival curve of indicated mice with 5-FU (150 mg/kg) via intraperitoneal injections every 7 days for two rounds. Data obtained from 8 mice in each group. *P* values determined by Log-rank (Mantel-Cox) test. (G) (Top) Poisson statistical analysis from the limiting dilution assays. Symbols represent the percentage of negative mice for each dose of cells. Solid lines indicate the best-fit linear model for each dosage. Dotted lines represent 95% Confidence Intervals. (Bottom) Frequencies of functional hematopoietic stem cells (HSC) were calculated according to Poisson statistics. (H) Quantification of donor-derived PB cells at the indicated time points after competitive transplantation. Data obtained from 8 mice in each group. *P* value determined by two-way ANOVA. (I) Quantification of donor-derived BM cells of indicated mice 24 weeks after competitive transplantation. Data presented as mean±SD from 8 mice in each group. (J) Quantification of donor-derived LSK and SLAM-LSK cells of indicated mice as in (I). Data presented as mean±SD from 8 mice in each group. All *P* values determined by unpaired two-tailed Student *t* test unless otherwise indicated. See also *Online Supplementary Figures S1, S2* for supporting Information. CRU: competitive repopulating units (long-term repopulating hematopoietic stem cells).

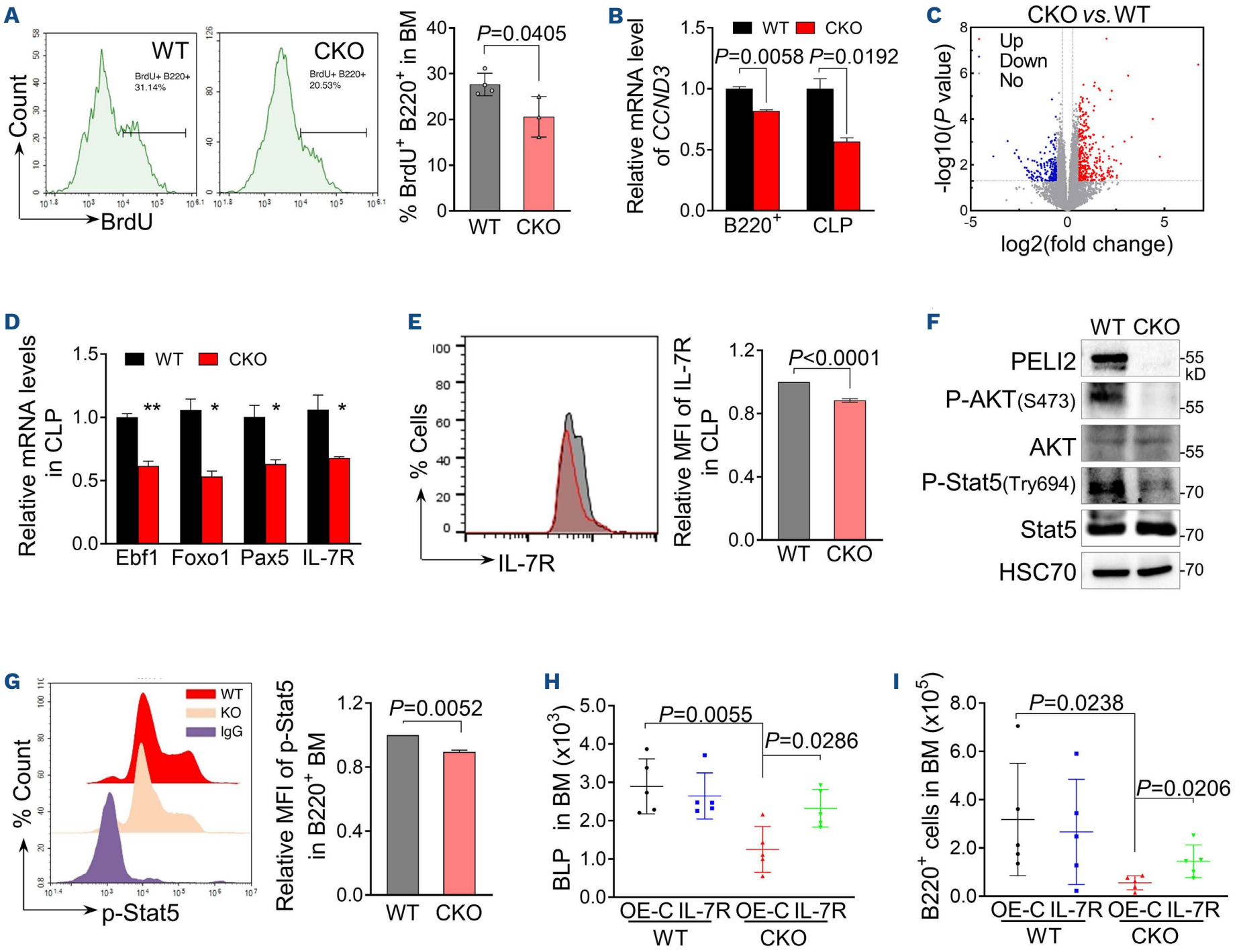

Figure 3. *PELI2* regulated early B-cell development through IL-7R signaling. (A) Proliferation analysis of bone marrow (BM) B cells (B220⁺) from indicated mice. 8-week old mice were injected intraperitoneally with BrdU for 3 hours. BM cells were collected and stained with anti-B220 antibodies in combination with BrdU detection methodology. Percentages in the bar graph indicate BrdU-positive cells in the gated B220⁺ cells. Each dot represents one mouse. Data presented as mean±Standard Deviation (SD). WT: wild-type. (B) Quantification of mRNA expression of *CCND3* in the common lymphoid progenitors (CLP) and B220⁺ cells from BM of WT and hematopoietic-specific *PELI2* knockout (*PELI2*^{CKO}) mice (CKO). Data presented as mean±SD from 3 independent experiments. (C) BM B220⁺ cells isolated from 8-week-old WT and *PELI2*^{CKO} mice and analyzed by RNA sequencing. Volcano plot of the differentially expressed genes between WT and *PELI2*^{CKO} BM B220⁺ cells are shown. (D) Quantification of mRNA expression of *Ebf1*, *Foxo1*, *Pax5*, and *IL-7R* expression in the BM CLP cells of WT and *PELI2*^{CKO} mice. Data presented as mean±SD from 3 independent experiments. **P*<0.05; ***P*<0.01. (E) Flow cytometric analysis of cell surface expression of IL-7R in the BM CLP cells of indicated mice. (Right) Quantification of mean fluorescence intensity (MFI) of IL-7R. Data presented as mean±SD from 3 independent experiments. (F) Immunoblotting analysis of indicated proteins in B220⁺ BM B cells from indicated mice. HSC70 was used as loading control. (G) Flow cytometric analysis of intracellular Stat5 phosphorylation in cells as in (F) except the cells were treated with IL-7 (50 ng/mL) for 30 minutes. (Right) Quantification of mean fluorescence intensity (MFI) of phosphorylated Stat5. Data presented as mean±SD from 3 independent experiments. (H and I) Quantification of B-cell-biased lymphoid progenitor (BLP) cells and B220⁺ cells in BM from mice transplanted with WT and *PELI2*^{CKO} cKit⁺ BM cells transduced with lentivirus expressing IL-7R or blank vector (OE-C) at one month post transplantation. Each dot represents one mouse. Data presented as mean±SD. All *P* values were determined by unpaired two-tailed Student *t* test unless otherwise indicated. See also *Online Supplementary Figure S4* for supporting information.

expression was transcriptionally repressed in *PELI2*^{CKO} mice (*Online Supplementary Figure S5A*). In addition, *PELI2* overexpression protected PU.1 from the time-dependent degradation upon cycloheximide (CHX) treatment (*Online Supplementary Figure S5B*).

Considering *PELI2* is an E3 ubiquitin ligase, we speculated that *PELI2* promotes PU.1 stability via ubiquitination. Co-immunoprecipitation (Co-IP) assays demonstrated an

interaction between *PELI2* and PU.1 (Figure 4B). To map the domains that are critical for the interaction of *PELI2* and PU.1, we constructed a series of truncated forms of the two proteins (Figure 4C, E). Co-IP assays with these truncations revealed that the *PELI2* FHA domain was responsible for the interaction with the PEST domain of PU.1 (Figure 4D, F). Overexpression of *PELI2* promoted K63-linked ubiquitination of PU.1 (*Online Supplementary Figure S5C*), whereas similar approaches using K48-linked ubiquitin failed to detect any increase in ubiquitination of PU.1 (*Online Supplementary Figure S5D*). In line with this, a reduction in K63-linked ubiquitination but an increase in K48-linked ubiquitin of PU.1 were observed in $B220^+$ BM cells from $PELI2^{CKO}$ mice (Figure 4G). These data demonstrated that *PELI2* regulates PU.1 protein stability via K63-linked ubiquitination.

PU.1 induced a marked increase in luciferase activity in HEK293T cells transduced with *IL-7R* promoter, which was further enhanced by *PELI2* overexpression (*Online Supplementary Figure S5E*). We then analyzed chromatin occupancy of PU.1 on the *IL-7R* promotor region by ChIP, and found that the binding of PU.1 to the *IL-7R* promoter was significantly reduced in $B220^+$ BM cells upon *PELI2* deletion (Figure 4H). Importantly, PU.1 overexpression significantly restored the reduced IL-7R expression, which successfully reversed the impaired pre-B CFU formation of BM Lin^- cells from $PELI2^{CKO}$ mice (Figure 4 I, *Online Supplementary Figure S5F*). Similar rescue for the defect of B-cell differentiation was also observed in CKO mice with PU.1 overexpression (*Online Supplementary Figure S6*). Collectively, these data demonstrated that *PELI2* promotes PU.1 stability via K63-linked ubiquitination to regulate IL-7R expression, which is required for early B-cell development.

PELI2 regulated cell proliferation via IL-7R signaling in B-cell precursor acute lymphoblastic leukemia cells

Given that *PELI2* is essential for IL-7R expression, we assessed whether *PELI2* plays important roles in the progression of BCP-ALL characterized by excessively activating IL-7R signaling.[17,18] We first analyzed the published RNA sequencing data from patients with BCP-ALL, and found that *PELI2* is highly expressed in parallel with IL-7R expression in PB samples obtained from 23 BCP-ALL patients compared with the corresponding normal individuals (*Online Supplementary Figure S7A*). Consistent with this, our independent assays with BM mononuclear cells from 7 BCP-ALL patients also revealed a significant upregulation of *PELI2* expression and positive correlation with IL-7R (Figure 5A, B), which was confirmed by the increase in both protein levels in the primary BCP-ALL cells (Figure 5C).

We next utilized a BCP-ALL cell line Nalm-6 to explore the roles of *PELI2* in BCP-ALL. PELI2 knockdown led to a marked reduction in IL-7R expression (*Online Supplementary Figure S7B*), thereby inhibiting its downstream signaling including the phosphorylation of AKT and ERK, cMyc (Figure 5D). Indeed, silencing of *PELI2* dramatically inhibited the proliferation of Nalm-6 cells and 697 cells in BCP-ALL cells (Figure 5E, *Online Supplementary Figure S7C*). This was further confirmed by the down-regulated expression of *Ki67* and repressed DNA replication in Nalm-6 cells transduced with *PELI2* shRNA (Figure 5F, *Online Supplementary Figure S7D*). Similarly, *PELI2* knockdown also significantly reduced the colony formation ability of primary BCP-ALL $CD34^+$ cells (Figure 5G). On the contrary, ectopic expression of *PELI2* promoted the IL-7R signaling and proliferation of Nalm-6 cells (*Online Supplementary Figure S7E, F*), and even attenuated the effect of vincristine chemotherapy on Nalm-6 cells (*Online Supplementary Figure S7G*). Notably, overexpression of IL-7R effectively reverted the inhibitory proliferation of Nalm-6 cells induced by *PELI2* knockdown *in vitro* (Figure 5H). These findings suggested that *PELI2* regulates cell proliferation via IL-7R signaling in BCP-ALL cells.

TCF3 was required for the IL-7R expression in B-cell precursor acute lymphoblastic leukemia cells

Given our finding that PU.1 is relatively unaffected or undetectable in BCP-ALL (Figure 5C, *Online Supplementary Figure S7A*), we screened 26 transcription factors (TF) of *IL-7R* predicted from 3 independent databases (*Online Supplementary Figure S8A*). Among those highly expressed in BCP-ALL, TCF3 knockdown led to a significant reduction in IL-7R expression (Figure 6A, *Online Supplementary Figure S8B*), indicating that TCF3 is required for IL-7R expression in Nalm-6 cells. Similarly, TCF3 was positively correlated with the expression of *PELI2* and IL-7R in BCP-ALL (Figure 6B, *Online Supplementary Figure S8C, D*), which is consistent with the elevated protein level in BM cells from BCP-ALL patients (Figure 5C). Furthermore, TCF3 knockdown inhibited the proliferation of Nalm-6 cells, which phenocopied the effects of *PELI2* silencing (*Online Supplementary Figure S8E*).

Silencing of *PELI2* led to a dramatic reduction in TCF3, while its ectopic expression resulted in an increase in TCF3 protein level (*Online Supplementary Figure S8F, G*). Importantly, overexpression of TCF3 effectively restored the IL-7R expression and subsequent Nalm-6 cell growth inhibited by *PELI2* silencing (Figure 6C, D), suggesting that TCF3 mediated the regulation of *PELI2* on the Nalm-6 cell proliferation via IL-7R expression.

To reveal the regulation of TCF3 on IL-7R expression, we performed the luciferase reporter assays in HEK293T cells driven by *IL-7R* promoter. Overexpression of TCF3 induced a marked increase in luciferase activity, which was enhanced by *PELI2* overexpression (*Online Supplementary Figure S8 I*). The binding of TCF3 on the *IL-7R* promoter was further confirmed by ChIP analysis in which *PELI2* knockdown greatly reduced their interaction in Nalm-6 cells (Figure 6E). Collectively, these data demonstrated the *PELI2*-TCF3 axis regulates IL-7R expression, which is required for the proliferation of BCP-ALL cells.

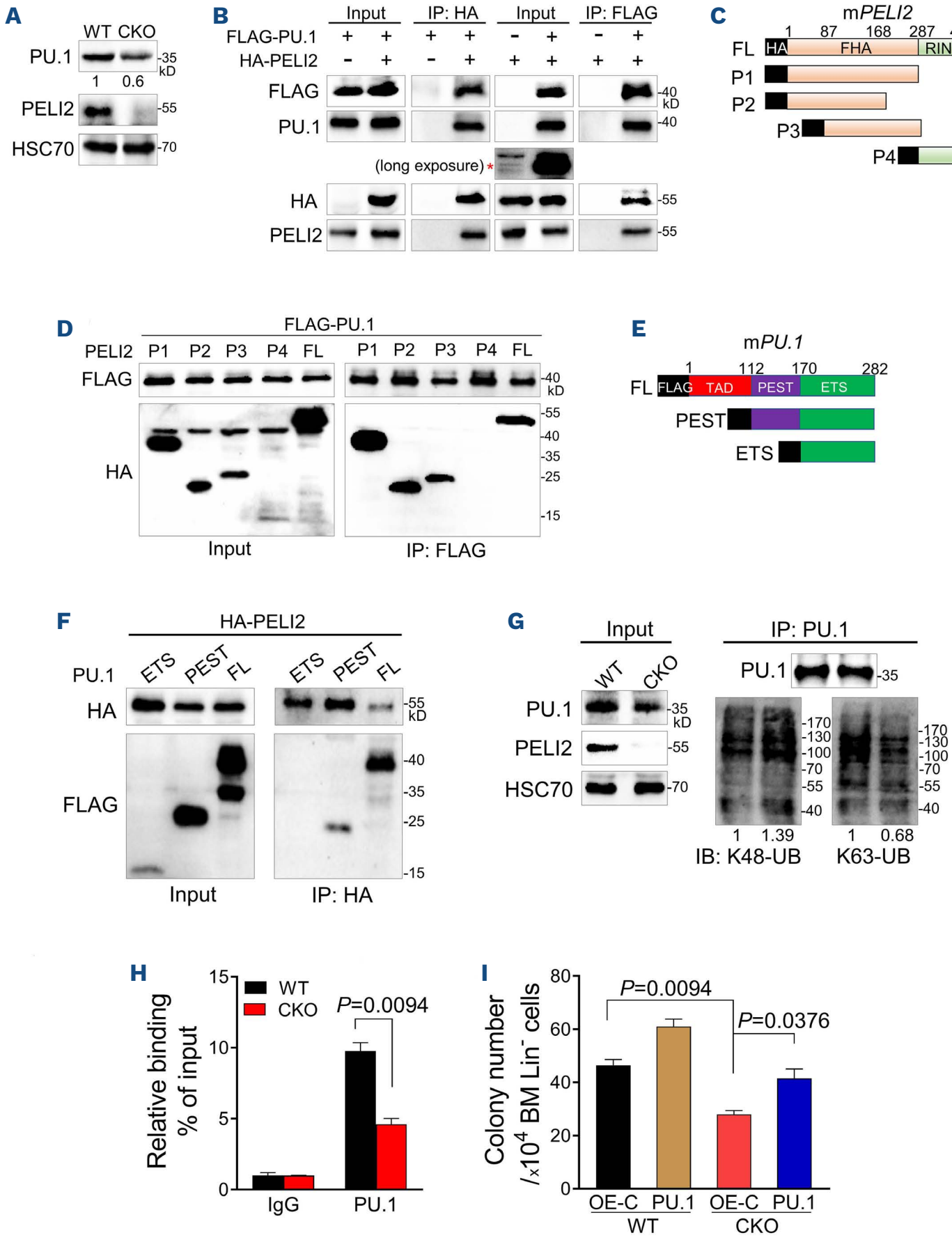

Figure 4. *PELI2* regulated IL-7R expression via protecting PU.1 from degradation in normal B-cell development. (A) Immunoblotting analysis of PU.1 protein level in B cells purified from bone marrow (BM) of wild-type (WT) and hematopoietic-specific *PELI2* knockout mice (*PELI2*^{CKO}) mice. HSC70 was used as loading control. Numbers indicate the relative band intensity of PU.1 that normalized to HSC70. (B) Reciprocal co-immunoprecipitation (Co-IP) of exogenous FLAG-mouse PU.1 and HA-mouse *PELI2* in HEK293T cells. Bands obtained from independent membranes blotted with indicated antibodies. (C) Structure of full-length and truncated mouse *PELI2*. (D) Co-IP analysis of *PELI2* mutants binding to PU.1. HEK293T cells were co-transfected with mouse *PELI2* truncations (HA tagged) and FLAG-mouse PU.1, and IP analysis was performed with anti-FLAG antibody. (E) Structure of full-length and truncated mouse PU.1. (F) Co-IP analysis of PU.1 mutants binding to *PELI2*. HEK293T cells were co-transfected with mouse PU.1 truncations (FLAG tagged) and HA-mouse *PELI2*, and IP analysis was performed with anti-HA antibody. (G) Immunoblotting analysis of ubiquitination of PU.1 immunoprecipitated from BM B cells of WT and *PELI2*^{CKO} mice with K63-linkage and K48-linkage specific polyubiquitin antibodies. Numbers indicate the relative band intensity of the ubiquitin blots to WT. (H) Chromatin IP analyses of promoter binding activity of PU.1 to *IL-7R* in BM B220^{+} cells from WT and *PELI2*^{CKO} mice. Data presented as mean±Standard Deviation (SD) from 3 independent experiments. (I) Pre-B colony formation assays of BM lineage^{-} cells from WT and *PELI2*^{CKO} mice transduced with lentivirus expressing PU.1 or blank vector (OE-C). Colony number was quantified. Data presented as mean±SD from 3 independent experiments. All *P* values determined by unpaired two-tailed Student *t* test unless otherwise indicated. See also *Online Supplementary Figures S5, S6* for supporting information.

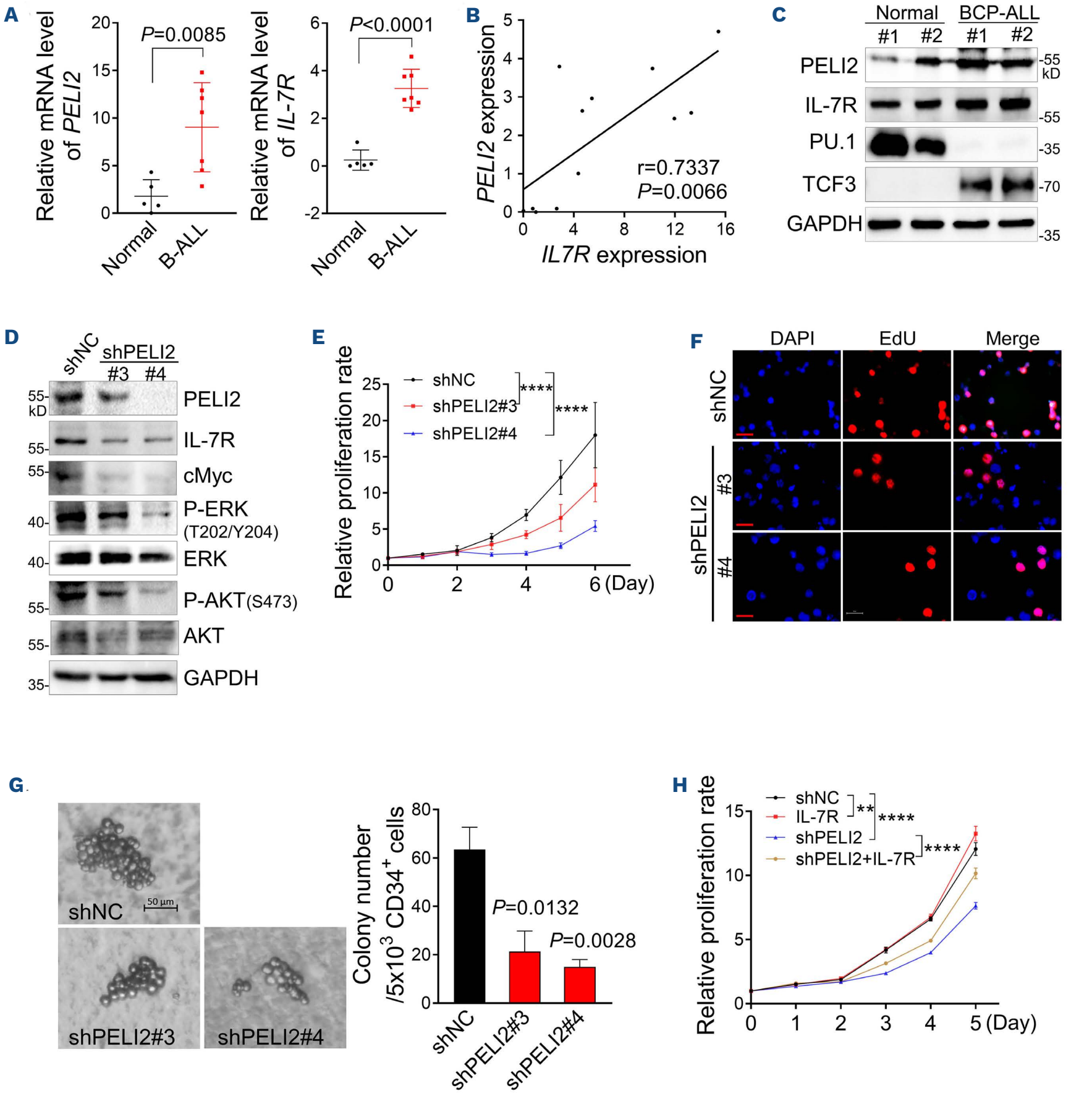

Figure 5. *PELI2* was required for the cell proliferation via IL-7R signaling in B-cell precursor acute lymphoblastic leukemia cells. (A) Quantification of mRNA expression of *PELI2* and *IL-7R* in the bone marrow mononuclear cells from primary B-cell precursor acute lymphoblastic leukemia (BCP-ALL) patients and healthy donors. Each dot represents one mouse. Data presented as mean± Standard Deviation (SD). (B) Correlation of *PELI2* expression with IL-7R in (A). Pearson's correlation coefficient (r) and paired *t* test *P* values are shown. (C) Immunoblotting analysis of indicated proteins in the bone marrow mononuclear cells from primary BCP-ALL patients and healthy donors. GAPDH was used as loading control. (D) Immunoblotting analysis of indicated proteins in Nalm-6 cells transduced with retroviruses encoding indicated shRNA. shNC represents a non-targeting shRNA. GAPDH was used as loading control. (E) Statistical analysis of cell proliferation in Nalm-6 cells as in (D). Data obtained from 3 independent experiments. *P* value determined by two-way ANOVA. ****$P<0.0001$. (F) Nalm-6 cells as in (D) were labeled with EdU for 2 hours and stained with azide-conjugated Alexa567 (red fluorescence) and DAPI (blue fluorescence). Scale bar: 20 μm. (G) Primary BCP-ALL bone marrow $CD34^+$ cells with *PELI2* knockdown were subjected to colony-forming unit assays. (Left) Representative colony morphology on day 14. Colony number was quantified. shNC represents a non-targeting shRNA. Data presented as mean±SD from 3 independent experiments. (H) Statistical analysis of cell proliferation in Nalm-6 cells transduced with retroviruses encoding indicated shRNA in the presence of IL-7R overexpression. Data obtained from 3 independent experiments. *P* value determined by two-way ANOVA. **$P<0.01$; ****$P<0.0001$. All *P* values determined by unpaired two-tailed Student *t* test unless otherwise indicated. See also *Online Supplementary Figure S7* for supporting information.

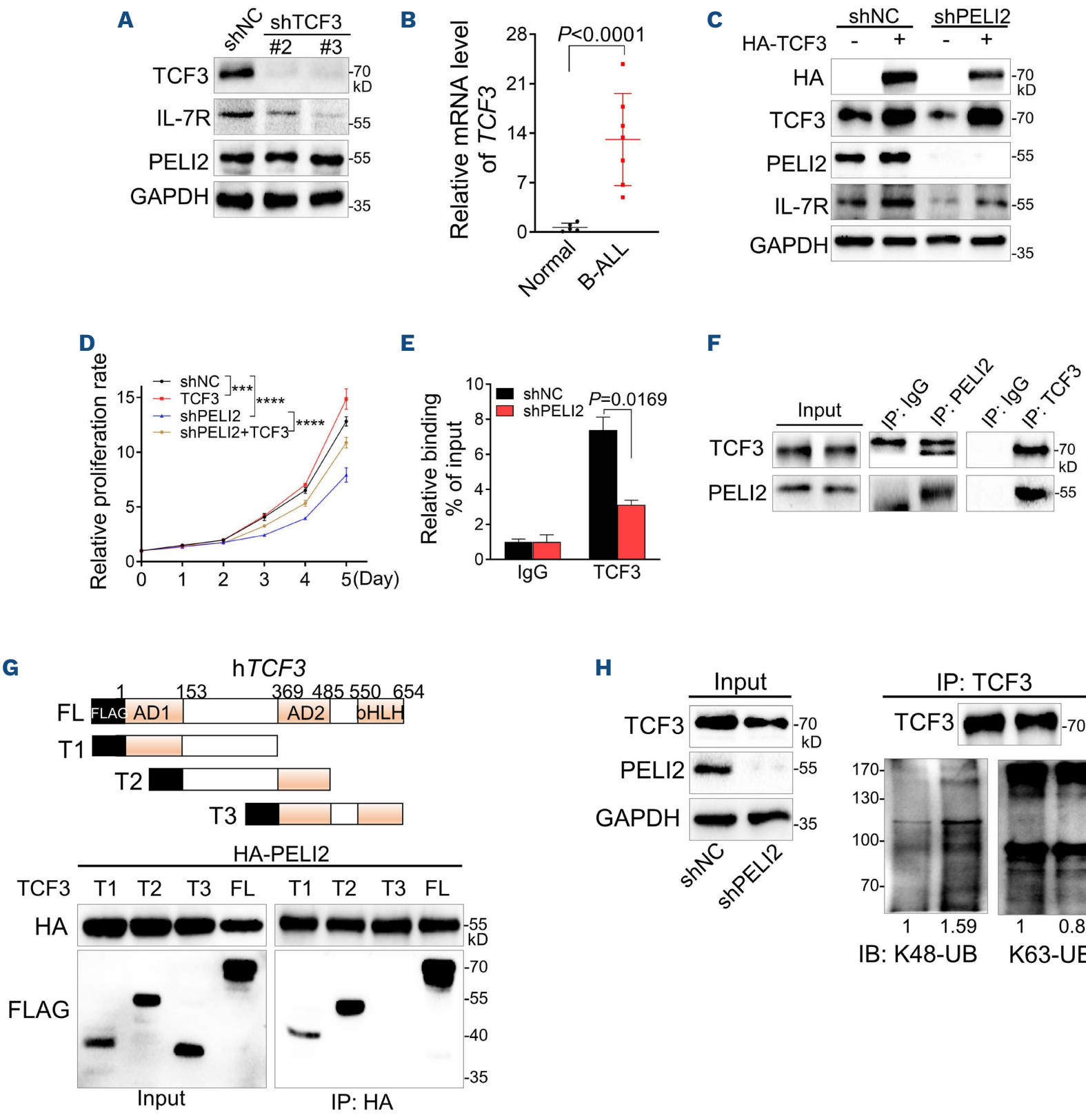

Figure 6. *PELI2* stabilized TCF3 via K63-linked polyubiquitination to regulate IL-7R expression in B-cell precursor acute lymphoblastic leukemia cells. (A) Immunoblotting analysis of IL-7R and *PELI2* expression in Nalm-6 cells transduced with retroviruses encoding indicated shRNA. shNC represents a non-targeting shRNA. GAPDH was used as loading control. (B) Statistical analysis of *TCF3* mRNA level in the bone marrow mononuclear cells as in Figure 5A (each dot represents one sample). (C) Immunoblotting analysis of indicated proteins in Nalm-6 cells transduced with retroviruses encoding indicated shRNA in the presence of TCF3 overexpression. shNC represents a non-targeting shRNA. GAPDH was used as loading control. (D) Statistical analysis of cell proliferation in Nalm-6 cells as in (C). Data obtained from 3 independent experiments. *P* value determined by two-way ANOVA. ***$P<0.001$; ****$P<0.0001$. (E) Chromatin immunoprecipitation analyses of promoter binding activity of TCF3 to *IL-7R* in Nalm-6 cells transduced with retroviruses encoding indicated shRNA. shNC represents a non-targeting shRNA. Data presented as mean± Standard Deviation (SD) from 3 independent experiments. (F) Co-immunoprecipitation (Co-IP) analysis of endogenous *PELI2* and TCF3 in Nalm-6 cells. (G) Structure of full-length and truncated human TCF3. Co-IP analysis of TCF3 mutants binding to *PELI2*. HEK293T cells were co-transfected with TCF3 truncations (FLAG tagged) and HA-*PELI2*, and IP analysis was performed with anti-HA antibody. (H) Immunoblotting analysis of ubiquitination of TCF3 immunoprecipitated from Nalm-6 cells transduced with indicated retroviruses with K63-linkage and K48-linkage specific polyubiquitin antibodies. shNC represents a non-targeting shRNA. Numbers indicate the relative band intensity of the ubiquitin blots to corresponding control. All *P* values determined by unpaired two-tailed Student *t* test unless otherwise indicated. See also *Online Supplementary Figures S8, S9* for supporting information.

PELI2 promoted TCF3 protein stability via K63-linked polyubiquitination in B-cell precursor acute lymphoblastic leukemia cells

Based on the observed correlation of TCF3 protein level with *PELI2* expression, we sought to determine whether *PELI2* regulates TCF3 protein level via ubiquitination similar to PU.1. Indeed, upon CHX treatment, TCF3 protein stability was reduced in Nalm-6 cells with PELI2 knockdown compared to control groups (*Online Supplementary Figure S9A*), while enhanced protein stability was observed in Nalm-6 cells with *PELI2* overexpression (*Online Supplementary Figure S9B*). Furthermore, the decrease in TCF3 protein induced by *PELI2* knockdown was clearly abolished by the pre-treatment of MG132 (*Online Supplementary Figure S9C*). Co-IP analysis demonstrated an interaction between *PELI2* and TCF3 in HEK293T cells (*Online Supplementary Figure S9D*). Their interaction was confirmed by endogenous co-IP in Nalm-6 cells (Figure 6F). Furthermore, *PELI2*-binding domain in TCF3 was mapped to the interval between AD1 and AD2 domains (Figure 6G), and the FHA domain of *PELI2* is responsible for the TCF3-binding (*Online Supplementary Figure S9E*) indicated by Co-IP experiments.

Overexpression of *PELI2* promoted K63-linked ubiquitination of TCF3 (*Online Supplementary Figure S9F*), whereas similar approaches using K48-linked ubiquitin failed to detect any increase in ubiquitination of TCF3 (*Online Supplementary Figure S9G*). In line with this, we also observed that K63-ubiquitination of endogenous TCF3 was increased upon the overexpression of *PELI2* in Nalm-6 cells. Conversely, *PELI2* knockdown led to the reduced K63-ubiquitination but increased K48-ubiquitination of TCF3 in Nalm-6 cells (Figure 6H, *Online Supplementary Figure S9H*).

PELI2 inhibition reduced the leukemia burden in human B-cell precursor acute lymphoblastic leukemia xenograft mice

To assess the effect of *PELI2* repression on tumor progression of BCP-ALL, we established *PELI2*-silencing Nalm-6 cell lines using retroviral construct expressing shRNA targeting *PELI2*, and transplanted these cells into immunocompromised NOD scid gamma (NSG) mice (Figure 7A). All Nalm-6-bearing mice died at around 26 days, whereas the mice bearing *PELI2*-silencing Nalm-6 exhibited significantly prolonged median survival (Figure 7B).

As previously reported,[27] Nalm-6-bearing mice exhibited rapid tumor burden and cell infiltration in spleen and BM. Compared with control Nalm-6-bearing mice, the spleen size of mice bearing *PELI2*-silencing Nalm-6 was significantly reduced (Figure 7C, D). Nalm-6 cell frequencies were much lower in these mice compared to controls (Figure 7E). Consistent with the role of TCF3 in mediating IL-7R expression and BCP-ALL cell proliferation *in vitro*, its overexpression aggravated the progression of Nalm-6-driven BCP-ALL *in vivo* (Figure 7B, *Online Supplementary Figure S10A*). Notably, replenishment of TCF3 significantly reversed the suppression phenotypes of mice bearing *PELI2*-silencing Nalm-6, including the shorter survival (Figure 7B), enlarged spleen (Figure 7C, D), and aggravated infiltrating Nalm-6 cells in spleen and BM (Figure 7E). A similar reversal of *PELI2* inhibition-induced suppression phenotypes of Nalm-6-driven BCP-ALL was also observed in mice bearing *PELI2*-silencing Nalm-6 with IL-7R overexpression (*Online Supplementary Figure S10B-F*).

We also performed the xenotransplantation experiment to determine the *in vivo* effect of *PELI2* inhibition on the progress of human BCP-ALL. Primary human BCP-ALL mononuclear cells were transduced with *PELI2* shRNA and then transplanted into NSG mice. Compared to the poor survival in the control group, *PELI2*-knockdown significantly prolonged the survival of BCP-ALL-bearing mice (Figure 7F). Furthermore, *PELI2* silencing led to a significant reduction in the frequency of human leukemic blasts in the BM and spleen in recipient mice at two months post transplantation (Figure 7G). These results indicated that *PELI2* inhibition reduced the human BCP-ALL burden *in vivo*.

Discussion

IL-7R signaling mainly controls the proliferation and survival of early B-cell progenitor cells in normal B-cell development.[28] Our study demonstrated that *PELI2* promotes PU.1 stability via ubiquitination to regulate IL-7R expression. Loss of *PELI2* leading to the degradation of PU.1, which in turn down-regulated the IL-7R expression, impaired the commitment and proliferation of early B-cell progenitors (Figure 8), whereas T-lineage differentiation was unaffected. This is consistent with the critical role of PU.1 in IL-7R expression, which specifically occurred in B-cell lineages but not T-cell lineages.[26,29] Given that IL-7R is essential for lymphoid development, it is reasonable to suppose that the differing commitment of CLP relies on the available transcription factors of IL-7R. In line with this, an upstream regulatory element of PU.1 functions as a PU.1 enhancer in B cells but as a repressor in T-cell precursors.[30]

Our data demonstrated that *PELI2* functions as a key mediator at the transition from the CLP to the earliest stage of B-cell specification via PU.1, which is consistent with the role of PU.1 in early lymphopoiesis, the deficiency of which led to the compromised differentiation of CLP into BLP.[31] In addition, PU.1 is also required for the developmental progression of CLP from LMPP, the deficiency of which leads to the reduced CLP and consequent B-cell development.[31,32] Given that *PELI2* deletion led to reduced numbers of CLP, we cannot exclude the possibility that loss of *PELI2* disrupts the transition of early lymphoid progenitors LMPP to CLP via PU.1.

Although the frequency of HSC in *PELI2*^{CKO} mice BM is comparable to that of WT controls, *PELI2*^{CKO} HSC exhibited notably impaired self-renewal and reconstitution upon the

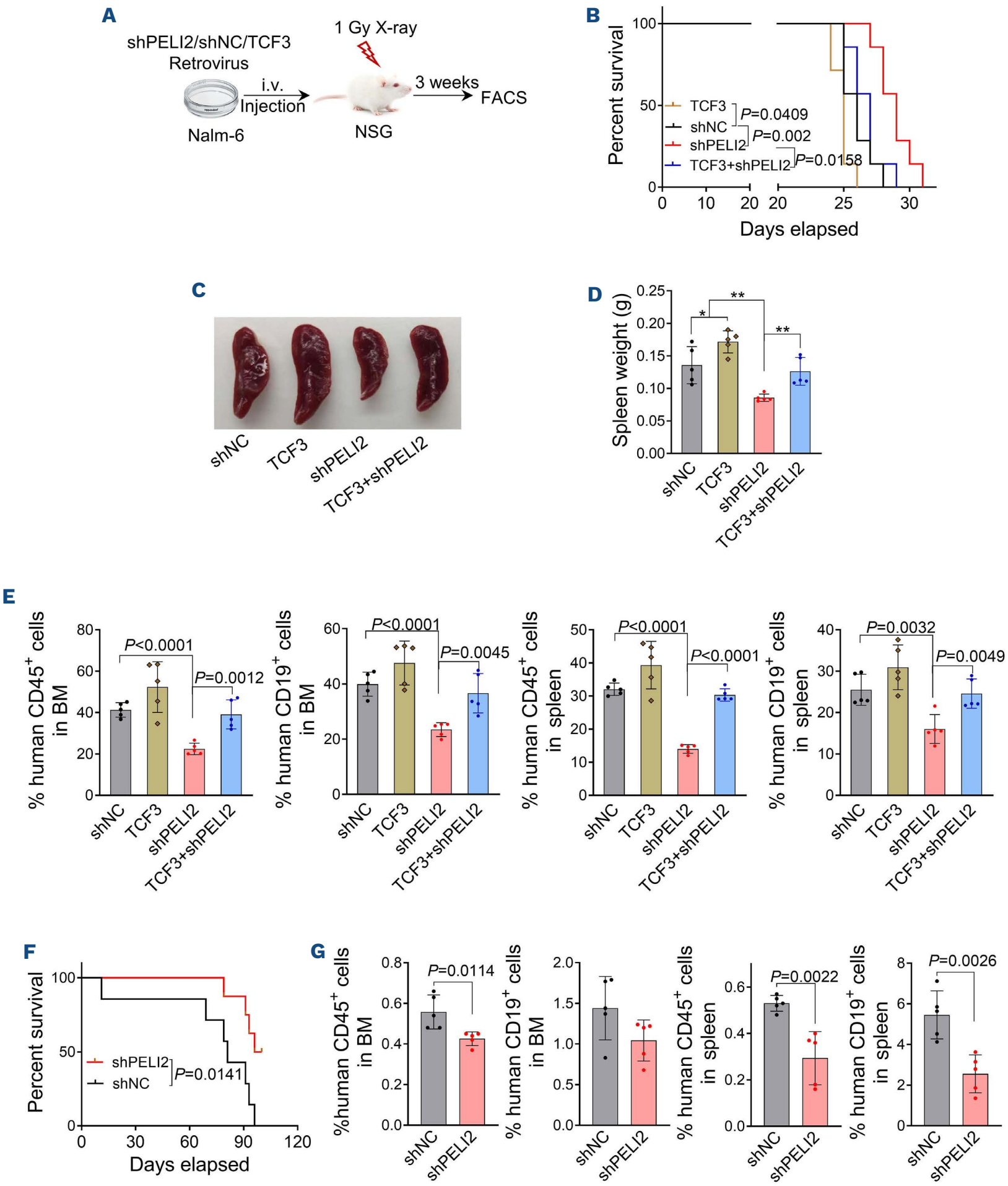

Figure 7. *PELI2* inhibition reduced leukemia burden in the human B-cell precursor acute lymphoblastic leukemia xenograft. (A) Schematic representation of human BCP-ALL xenograft. Five million Nalm-6 cells, transduced with indicated retroviruses, were injected into irradiated NOD scid gamma (NSG) mice (1 Gy). shNC represents a non-targeting shRNA. (B) Kaplan-Meier survival curve of indicated Nalm-6-xenograft mice. Data obtained from 8 mice in each group. *P* values determined by Log-rank (Mantel-Cox) test. (C) Representative spleen of indicated mice as in (B). (D) Statistical analysis of spleen weight from mice in (C). Each dot represents one mouse. Data presented as mean±Standard Deviation (SD). **P*<0.05, ***P*<0.01. (E) Human CD45$^+$ and CD19$^+$ cells from bone marrow (BM) and spleen of indicated mice were analyzed by flow cytometry. Each dot represents one mouse. Data presented as mean±SD. (F) Kaplan-Meier survival curve of indicated patient-derived xenograft (PDX) mice. Data obtained from 7 mice in each group. *P* values determined by Log-rank (Mantel-Cox) test. (G) Human CD45$^+$ and CD19$^+$ cells from BM and spleen of indicated PDX mice were analyzed at two months post transplantation by flow cytometry. Each dot represents one mouse. Data presented as mean±SD. *P* values determined by unpaired two-tailed Student *t* test unless otherwise indicated. See also *Online Supplementary Figure S10* for supporting information.

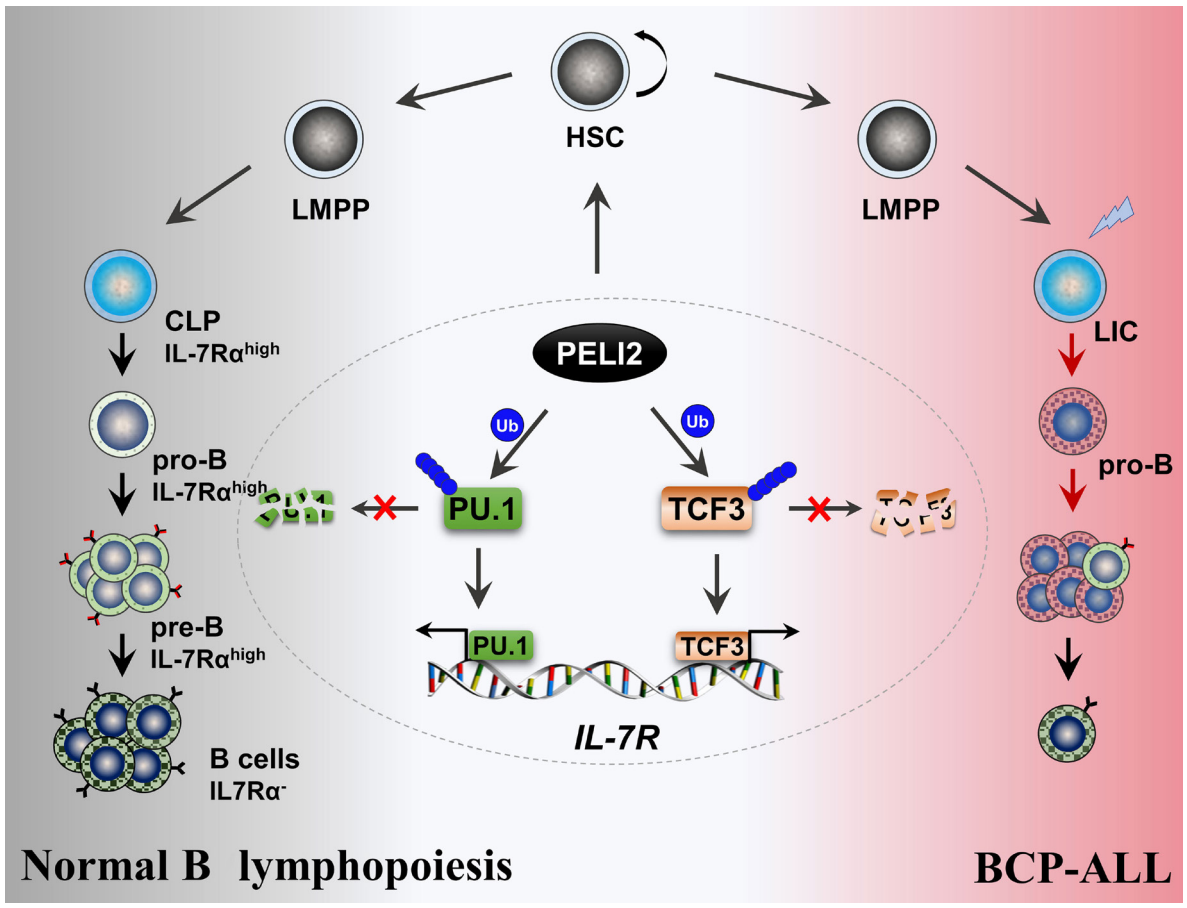

Figure 8. Schematic diagram illustrates the regulatory role of *PELI2* in normal B lymphopoiesis and B-cell precursor acute lymphoblastic leukemia. *PELI2* regulated early B-cell progenitor homeostasis and the progression of BCP-ALL by maintaining the IL-7R expression via the ubiquitination of PU.1 and TCF3, respectively.

challenge of 5-FU. This was further confirmed by the defects of functional HSC in the competitive transplantation and limiting dilution assays, indicating that *PELI2* is required for stressed hematopoiesis. Indeed, PU.1 is expressed in HSC and exhibits a gradual decrease during the subsequent differentiation into common lymphoid and myeloid progenitors.[33] PU.1 has also been identified as a master regulator in HSC cell fate decisions and homing through the interaction with a variety of regulatory factors.[34,35] Considering that PU.1 protects HSC from excessive exhaustion by controlling the transcription of multiple cell-cycle regulators,[36] *PELI2* may regulate HSC through PU.1 protein stability that is similar to its role in IL-7R expression during early B-cell progenitor commitment and proliferation. Given that the regulatory roles of *PELI2* in immunity and potential inflammatory modulation of hematopoiesis, there is also a possibility that the defects of functional HSC in *PELI2* knockout mice are feedback cues by the altered immunity induced by *PELI2* deletion.

Our study also provides strong rationales for targeting IL-7R for the treatment of BCP-ALL, which is characterized by a block in lymphoid differentiation leading to the accumulation of immature progenitor cells.[37] There is growing evidence indicating that excessive IL-7R signaling is oncogenic, being responsible for resistance to conventional chemotherapy and targeted therapeutics.[38-40] TCF3, a defined transcription factor in normal B-cell differentiation, is genetically altered via translocations, deletions or mutations in BCP-ALL,[5] leading to aberrant gene expression patterns in leukemic cells. Our data demonstrated that *PELI2* promotes TCF3 protein stability via ubiquitination that is required for the IL-7R expression in BCP-ALL cells (Figure 8). Indeed, TCF3 showed different expression with PU.1 during normal B-cell differentiation (*Online Supplementary Figure S8H*), which may account for its distinct requirement for IL-7R expression in BCP-ALL that occurs in late B-cell progenitor cells. Inhibition of *PELI2* suppressed the proliferation of BCP-ALL cells *in vitro* and *in vivo*. Therefore, the high expression of *PELI2* in BCP-ALL provides therapeutical benefit for targeting *PELI2* in the treatment of BCP-ALL.

In summary, we demonstrate that *PELI2* regulated early B-cell progenitor homeostasis and the progression of BCP-ALL by maintaining IL-7R expression via the ubiquitination of PU.1 and TCF3, respectively (Figure 8). Therefore, these findings provide not only a new insight into the pathogenic mechanism for B-cell precursor malignancies, but also a proof of principle that targeting *PELI2* restricts B-cell precursor expansion via IL-7R inhibition.

Disclosures

No conflicts of interest to disclose.

Contributions

BZ designed and guided research. YX, WQ and CZ performed the experiments. YX, QZ, YL, CZ and BZ analyzed the data. YX and BZ wrote the original draft. XW, AZ and JG collected the healthy donors and BCP-ALL patient samples. TS, JL, CL, YS and BZ reviewed and edited the manuscript. All authors have read and agreed to the published version of the manuscript.

Acknowledgments

We thank Prof. Chunyan Ji (Qilu Hospital of Shandong Uni-

versity) for the gift of the Nalm-6 cell line. We thank Prof. Jianrong Wang (Suzhou University) for the gift of the 697 cell line. We also thank the Translational Medicine Core Facility of Shandong University for the availability of consultation and instruments that supported this work.

Funding

This work was supported by grants from National Natural Science Foundation of China (81874294), Taishan Scholars Program (TSQN201812015), the program for Multidisciplinary Research and Innovation Team of Young Scholars of Shandong University (2020QNQT007) and the key Program of Natural Science Foundation of Shandong Province (ZR2022LSW027). This work was also supported by the National Key Research and Development Program (2019YFA0905402) and the program for Innovative Research Team in the University of Ministry of Education of China (N. IRT_17R68).

Data-sharing statement

Supporting data are available in the Online Supplementary Appendix. Microarray data are available at GEO under accession number GSE228984. The datasets used and/or analyzed during the current study are available from the corresponding author on reasonable request.

References

1. Boller S GR. The regulatory network of B-cell differentiation: a focused view of early B-cell factor 1 function. Immunol Rev. 2014;261(1):102-115.
2. Inlay MA, Bhattacharya D, Sahoo D, et al. Ly6d marks the earliest stage of B-cell specification and identifies the branchpoint between B-cell and T-cell development. Genes Dev. 2009;23(20):2376-2381.
3. Nutt SL, Kee BL. The transcriptional regulation of B cell lineage commitment. Immunity. 2007;26(6):715-725.
4. Busslinger M. Transcriptional control of early B cell development. Annu Rev Immunol. 2004;22:55-79.
5. Somasundaram R, Prasad MAJ, Ungerbäck J, Sigvardsson M. Transcription factor networks in B-cell differentiation link development to acute lymphoid leukemia. Blood. 2015;126(2):144-152.
6. Clark MR, Mandal M, Ochiai K, Singh H. Orchestrating B cell lymphopoiesis through interplay of IL-7 receptor and pre-B cell receptor signalling. Nat Rev Immunol. 2014;14(2):69-80.
7. Corfe SA, Paige CJ. The many roles of IL-7 in B cell development; mediator of survival, proliferation and differentiation. Semin Immunol. 2012;24(3):198-208.
8. Milne CD, Paige CJ. IL-7: a key regulator of B lymphopoiesis. Semin Immunol. 2006;18(1):20-30.
9. Pieper K, Grimbacher B, Eibel H. B-cell biology and development. J Allergy Clin Immunol. 2013;131(4):959-971.
10. Peschon JJ, Morrissey PJ, Grabstein KH, et al. Early lymphocyte expansion is severely impaired in interleukin 7 receptor-deficient mice. J Exp Med. 1994;180(5):1955-1960.
11. von Freeden-Jeffry U, Vieira P, Lucian LA, McNeil T, Burdach SE, Murray R. Lymphopenia in interleukin (IL)-7 gene-deleted mice identifies IL-7 as a nonredundant cytokine. J Exp Med. 1995;181(4):1519-1526.
12. Dias S, Silva HJ, Cumano A, Vieira P. Interleukin-7 is necessary to maintain the B cell potential in common lymphoid progenitors. J Exp Med. 2005;201(6):971-979.
13. Kikuchi K, Lai AY, Hsu CL, Kondo M. IL-7 receptor signaling is necessary for stage transition in adult B cell development through up-regulation of EBF. J Exp Med. 2005;201(8):1197-1203.
14. Yao Z, Cui Y, Watford WT, et al. Stat5a/b are essential for normal lymphoid development and differentiation. Proc Natl Acad Sci U S A. 2006;103(4):1000-1005.
15. Chou W-C, Levy DE, Lee C-K. STAT3 positively regulates an early step in B-cell development. Blood. 2006;108(9):3005-3011.
16. Barata JT, Durum SK, Seddon B. Flip the coin: IL-7 and IL-7R in health and disease. Nat Immunol. 2019;20(12):1584-1593.
17. Almeida ARM, Neto JL, Cachucho A, et al. Interleukin-7 receptor α mutational activation can initiate precursor B-cell acute lymphoblastic leukemia. Nat Commun. 2021;12(1):7268.
18. Thomas KR, Allenspach EJ, Camp ND, et al. Activated interleukin-7 receptor signaling drives B-cell acute lymphoblastic leukemia in mice. Leukemia. 2022;36(1):42-57.
19. Humphries F, Bergin R, Jackson R, et al. The E3 ubiquitin ligase Pellino2 mediates priming of the NLRP3 inflammasome. Nat Commun. 2018;9(1):1560.
20. Berndsen CE, Wolberger C. New insights into ubiquitin E3 ligase mechanism. Nat Struct Mol Biol. 2014;21(4):301-307.
21. Xu Y, Zhao B. Research progress on E3 ubiquitin ligase Pellino proteins. Xiamen Univ Nat Sci. 2022;61(3):402-414.
22. Humphries F, Moynagh PN. Molecular and physiological roles of Pellino E3 ubiquitin ligases in immunity. Immunol Rev. 2015;266(1):93-108.
23. Bhansali RS, Rammohan M, Lee P, et al. DYRK1A regulates B cell acute lymphoblastic leukemia through phosphorylation of FOXO1 and STAT3. J Clin Invest. 2021;131(1):e135937.
24. Lu Z, Huang L, Li Y, et al. Fine-tuning of cholesterol homeostasis controls erythroid differentiation. Adv Sci (Weinh). 2022;9(2):e2102669.
25. Xiong Z, Xia P, Zhu X, et al. Glutamylation of deubiquitinase BAP1 controls self-renewal of hematopoietic stem cells and hematopoiesis. J Exp Med. 2020;217(2):e20190974.
26. DeKoter RP, Lee H-J, Singh H. PU.1 regulates expression of the interleukin-7 receptor in lymphoid progenitors. Immunity. 2002;16(2):297-309.
27. Tipanee J, Samara-Kuko E, Gevaert T, Chuah MK, VandenDriessche T. Universal allogeneic CAR T cells engineered with Sleeping Beauty transposons and CRISPR-CAS9 for cancer immunotherapy. Mol Ther. 2022;30(10):3155-3175.
28. Miller JP, Izon D, DeMuth W, Gerstein R, Bhandoola A, Allman D. The earliest step in B lineage differentiation from common lymphoid progenitors is critically dependent upon interleukin 7. J Exp Med. 2002;196(5):705-711.
29. Anderson MK, Hernandez-Hoyos G, Diamond RA, Rothenberg EV. Precise developmental regulation of Ets family transcription factors during specification and commitment to the T cell lineage. Development. 1999;126(14):3131-3148.
30. Rosenbauer F, Owens BM, Yu L, et al. Lymphoid cell growth and transformation are suppressed by a key regulatory element of the gene encoding PU.1. Nat Genet. 2006;38(1):27-37.

31. Pang SHM, de Graaf CA, Hilton DJ, et al. PU.1 is required for the developmental progression of multipotent progenitors to common lymphoid progenitors. Front Immunol. 2018;9:1264.
32. Iwasaki H, Somoza C, Shigematsu H, et al. Distinctive and indispensable roles of PU.1 in maintenance of hematopoietic stem cells and their differentiation. Blood. 2005;106(5):1590-1600.
33. Staber PB, Zhang P, Ye M, et al. The Runx-PU.1 pathway preserves normal and AML/ETO9a leukemic stem cells. Blood. 2014;124(15):2391-2399.
34. Etzrodt M, Ahmed N, Hoppe PS, et al. Inflammatory signals directly instruct PU.1 in HSCs via TNF. Blood. 2019;133(8):816-819.
35. Chavez JS, Rabe JL, Loeffler D, et al. PU.1 enforces quiescence and limits hematopoietic stem cell expansion during inflammatory stress. J Exp Med. 2021;218(6):e20201169.
36. Staber PB, Zhang P, Ye M, et al. Sustained PU.1 levels balance cell-cycle regulators to prevent exhaustion of adult hematopoietic stem cells. Mol Cell. 2013;49(5):934-946.
37. Mullighan CG. Molecular genetics of B-precursor acute lymphoblastic leukemia. J Clin Invest. 2012;122(10):3407-3415.
38. Cramer SD, Aplan PD, Durum SK. Therapeutic targeting of IL-7Ralpha signaling pathways in ALL treatment. Blood. 2016;128(4):473-478.
39. Cante-Barrett K, Spijkers-Hagelstein JA, Buijs-Gladdines JG, et al. MEK and PI3K-AKT inhibitors synergistically block activated IL7 receptor signaling in T-cell acute lymphoblastic leukemia. Leukemia. 2016;30(9):1832-1843.
40. Delgado-Martin C, Meyer LK, Huang BJ, et al. JAK/STAT pathway inhibition overcomes IL7-induced glucocorticoid resistance in a subset of human T-cell acute lymphoblastic leukemias. Leukemia. 2017;31(12):2568-2576.